Antiviral Research 231 (2024) 105993

Contents lists available at ScienceDirect

Antiviral Research

journal homepage: www.elsevier.com/locate/antiviral

Dynamic features of virus protein 1 and substitutions in the 3-phenyl ring determine the potency and broad-spectrum activity of capsid-binding pyrazolo[3,4-d]pyrimidines against rhinoviruses

Martina Richter [a,1], Maria Khrenova [b,c,1], Elena Kazakova [b], Olga Riabova [b], Anna Egorova [b], Vadim Makarov [b,*], Michaela Schmidtke [a,**]

[a] Jena University Hospital, Institute of Medical Microbiology, Section Experimental Virology, Hans-Knoell-Str. 2, 07743, Jena, Germany
[b] Federal Research Centre "Fundamentals of Biotechnology" of the Russian Academy of Sciences (Research Centre of Biotechnology RAS), 33-2 Leninsky Prospect, 119071, Moscow, Russia
[c] Department of Chemistry, Lomonosov Moscow State University, 1/3 Leninskie Gory, 119991, Moscow, Russia

ARTICLE INFO

Keywords:
Common cold
Antiviral
Pyrazolopyrimidine
OBR-5-340 derivatives
Spectrum of activity
Molecular dynamics
VP1

ABSTRACT

Pyrazolo[3,4-*d*]pyrimidines represent one potent class of well tolerated and highly active rhinovirus (RV) inhibitors that act as capsid binders. The lead compound OBR-5-340 inhibits a broad-spectrum of RVs. Aiming to improve lead activity, we evaluated the impact of structural modifications in the 3-phenyl ring of OBR-5-340 on its potency and spectrum of anti-RV activity *vitro*. Our results demonstrate the crucial role of substitution at position 4 for strong, broad-spectrum anti-RV activity. The 4-methyl (RCB23137) and 4-chloro (RCB23138) derivatives outperformed OBR-5-340 in terms of potency and anti-RV activity spectrum. Based on these findings, the compounds were selected for computational binding studies. Molecular dynamic simulations with six RVs differing in OBR-5-340, RCB23137, and RCB23138 sensitivity proved the impact of dynamic features of two VP1 loops enveloping these inhibitors on antiviral potency.

Rhinovirus (RV) species A, B, and *C* (80, 32, and 59 types, respectively) cause millions of mild acute respiratory infections, called common cold, annually (Esneau et al., 2022; Heikkinen and Jarvinen, 2003; Simmonds et al., 2020). RVs also considerably contribute to the burden of severe acute respiratory diseases including chronic bronchiolitis, pneumonia, exacerbation of chronic obstructive pulmonary disease, and asthma (Cilloniz et al., 2022; Esneau et al., 2022; Jackson and Gern, 2022; Lee et al., 2007; Lerman et al., 2023; Renwick et al., 2007; Royston and Tapparel, 2016; Ruuskanen et al., 2011). The mortality rate in patients admitted with RV infection was found to be nearly similar to that of infections with influenza A/B virus, respiratory syncytial virus, and metapneumovirus recently (Boon et al., 2024).

There is no direct-acting drug to treat RV-induced diseases today. Ideally, anti-RV medications should exert activity against all or at least the majority of RV types (broad-spectrum activity) because the circulation of a certain RV type is unpredictable (Esneau et al., 2022; Moriyama et al., 2020). A broad-spectrum anti-RV activity was shown for small molecules targeting the viral protease, RNA polymerase, and capsid proteins (Egorova et al., 2019; Patick, 2006; Rollinger and Schmidtke, 2011; Thibaut et al., 2016). Among the most promising leads of broad-spectrum capsid binders are pleconaril, vapendavir, and the pyrazolo[3,4-*d*]pyrimidine OBR-5-340 (Barnard et al., 2004; Feil et al., 2012; Groarke and Pevear, 1999; Makarov et al., 2015; Pevear et al., 1999). These inhibitors hinder RV adsorption and/or uncoating (Braun et al., 2015; Feil et al., 2012; Groarke and Pevear, 1999; Makarov et al., 2015; Wald et al., 2019). While pleconaril and vapendavir fit deeply within a small hydrophobic pocket in the canyon of the viral capsid protein 1 (VP1), the binding site of OBR-5-340 only partially coincides

Abbreviations: CC_{50}, 50% cytotoxic concentration; CPE, cytopathic effect; hpi, hours post infection; IC_{50}, 50% inhibitory concentration; MD, molecular dynamics; PCR, polymerase chain reaction; RV, rhinovirus; RT, reverse transcription; RVs, rhinoviruses; $TCID_{50}$, tissue culture infection dose 50%; VP1-4, virus capsid proteins 1-4.

** Corresponding author. Jena University Hospital, Department Medical Microbiology, Section Experimental Virology, Hans-Knoell-Str. 2, 07743, Jena, Germany.
* Corresponding author.
E-mail addresses: makarov@inbi.ras.ru (V. Makarov), michaela.schmidtke@med.uni-jena.de (M. Schmidtke).
[1] Shared first co-authorship: Martina Richter and Maria Khrenova contributed equally to the manuscript.

https://doi.org/10.1016/j.antiviral.2024.105993
Received 12 July 2024; Received in revised form 15 August 2024; Accepted 24 August 2024
Available online 3 September 2024
0166-3542/© 2024 The Authors. Published by Elsevier B.V. This is an open access article under the CC BY-NC-ND license (http://creativecommons.org/licenses/by-nc-nd/4.0/).

with them. OBR-5-340 shifts closer towards the pocket pore (Wald et al., 2019) what might explain the strong differences regarding inhibitor susceptibility found. Thus, pleconaril-insensitive RVs (naturally resistant), for example, rhinovirus B5 (RV-B5) are highly sensitive to OBR-5-340 (Richter et al., 2024; Wald et al., 2019). Using RV-B5 as example, we characterized the risk of resistance development (frequency and amino acids involved), suggested a molecular binding mechanism, and identified OBR-5-340 derivatives with structural modifications in position 4 of the 3-phenyl ring with strong inhibitory activity against OBR-5-340 escape mutants of RV-B5 (Richter et al., 2024). The impact of the studied structural modifications in the 3-phenyl ring on the antiviral activity against other RVs remained unclear.

Here, we analyzed the cytotoxicity and *in vitro* anti-RV activity (potency and spectrum) of the 10 derivatives from the RV-B5 study (Richter et al., 2024) against further 49 RV types (Supplementary Tables 1 and 2) aiming to identify derivatives with stronger and broader anti-RV activity than the lead OBR-5-340. Pleconaril was included as control. Molecular dynamics (MD) simulations with a set of six RV structures in complex with OBR-5-340 and two derivatives that outperformed OBR-5-340 in terms of potency and activity spectrum were applied to prove our hypothesis on the molecular base for the RV type-specific antiviral activity of these compounds. All Material and Methods are described in Supplementary Material 1.

The results on cytotoxicity (Table 1) and anti-RV activity (Table 2) of pleconaril and OBR-5-340 confirm published data (Ledford et al., 2004; Makarov et al., 2015). Overall 12% of the studied RV types (RV-B5, RV-B42, RV-A44, RV-B48, RV-A54) were insensitive to pleconaril in cytopathic effect inhibition assays in HeLa cells. OBR-5-340, was well tolerated and exerted high antiviral activity ($IC_{50} \leq 1$ μM) against these pleconaril-insensitive RVs. RV-A54, RV-A55, and RV-A64 were insensitive to OBR-5-340 (6% of the studied RV types of Table 2).

Our results obtained for the 10 OBR-5-340 derivatives clearly demonstrated a strong impact of modifications in the 3-phenyl ring on cytotoxicity and anti-RV activity (Tables 1 and 2, Supplementary Fig. 1). Both the position and the number of substituents in the 3-phenyl ring are important. Six of the ten derivatives, RCB04166 (R1 = R2 = H), RCB23139 (R1 = 4-Me, R2 = H), RCB23138 (R1 = 4-Cl, R2 = H), RCB23141 (R1 = 4-F, R2 = H), RCB23142 (R1 = H, R2 = 2-F), and RCB23144 (R1 = 4-F, R2 = 2-F) were well tolerated in HeLa and GMK cells (Table 1). In contrast to OBR-5-340, compounds RCB04166, RCB23142, and RCV23144 lack activity against the majority of tested RV types. The activity of RCB23141 resembled OBR-5-340. The moderately cytotoxic compound RCB23143 (R1 = 4-F, R2 = 3-F) also demonstrated strongly reduced anti-RV activity compared with 4-mono-substituted derivatives. Surprisingly, RCB23145 (R1 = 5-F, R2 = 3-F) acted slightly stronger compared with its structural isomers. Among 4-halogen-containing derivatives, RCB23139 (R1 = 4-Br, R2 = H) and RCB23140 (R1 = 4-I, R2 = H) showed the lowest 50% inhibitory concentration (IC_{50}) values for a wide range of RV types. However, when entering also cytotoxicity into activity evaluation RCB23137 and RCB23138 outperformed RCB23139 and RCB23140.

Importantly, RV-B5, -B42, -A44, -B48 and -B69, which were insensitive to pleconaril, were highly sensitive to all OBR-5-340 derivatives, regardless of substituents in the 3-phenyl ring.

Because some modifications rendered OBR-5-4-340 from ineffective to effective and *vice versa*, the anti-RV spectrum of activity was changed (Supplementary Fig. 1). In case of the RCB04166, RCB23139-145 it became narrower compared to OBR-5-340. In contrast, RCB23138 inhibited all except two of the RVs studied. RCB23137 inhibited all the RV tested, even the RV-A54, RV-A55, and RV-A64 that are insensitive to the parent OBR-5-340. The stronger and broader antiviral activity achieved by methyl (RCB23137) and chlorine (RCB23138) substitutions in position 4 of the 3-phenyl ring further proves that the addition of those substituents to the best-fit position can markedly improve target binding (Chiodi and Ishihara, 2023; Schonherr and Cernak, 2013). Because these derivatives also overcame OBR-5-340-resistance of RV-B5 mutants selected under treatment (Richter et al., 2024), we conclude that RCB23137 and/or RCB23138 might represent novel lead candidates for further anti-RV drug development. Beforehand, these compounds have to outperform OBR-5-340 also in terms of their pharmacokinetic and toxicity profile (Makarov et al., 2015) in future preclinical studies. Otherwise, further structure modification will be indicated.

Based on cryo-EM data on OBR-5-340 binding to VP1 (Wald et al., 2019) and MD simulations performed with RV-B5 and OBR-5-340-resistant variants thereof (Richter et al., 2024) we hypothesized that the correlated motion of two VP1 loops (VP1 192–195 and VP1 217–219) enveloping OBR-5-340 is required for strong anti-RV activity. Herein we checked the transferability of this hypothesis to i) another RV-B type and four RV-A types with distinct OBR-5-340 sensitivity and ii) to the two most potent OBR-5-340 derivatives RCB23137 and RCB23138. RV-B6 was included in our studies because of its markedly lower sensitivity to OBR-5-340 than RV-B5. Among RV-A types we chose the OBR-5-340-, RCB23137- and RCB23138-sensitive RV-A16 and RV-A18 and the OBR-5-340-insensitive RV-A55 and RV-A64. In contrast to RV-64, RV-A55 demonstrated binding with RCB23137 and RCB23138 as did RV-A16 and RV-A18. The distinct inhibitor sensitivity of the selected RV became even more visible in the dose-response curves shown together with the MD simulation results in Fig. 1A/B, 2A/B, and 3A/B.

Similarly to RV-B5 and OBR-5-340 ((Richter et al., 2024) and Fig. 1C here), we found for complexes with both RV-B5 and RV-B6 with RCB23137 or RCB23138 that the VP1 217–219 and VP1 192–195 loops belong to the same community (Fig. 1E–H). This community also included the inhibitor. RV-B6 demonstrated low affinity to OBR-5-340 (Table 2). The dynamic network analysis with RV-B6 and OBR-5-340 revealed a different community's composition. Here, the two VP1 loops belong to different communities; still each of these communities comprised a part of OBR-5-340 (Fig. 1D).

For the four RV-A types we identified similar structural fragments that are likely to envelope the inhibitor: VP1 184–186 and 211–214 fragments. For the OBR-5-340-, RCB23137- and RCB23138-sensitive RV-A16 and RV-A18 (Fig. 2A and B) we observed similar patterns of the dynamic behavior whereat both loops and the inhibitors belonged to the same community (Fig. 2C–E, G and H). The only exception was the RV-A18–RCB23137 complex: the loops were in the same community, while the inhibitor molecule belonged to a separate community not including protein fragments (Fig. 2F). The most challenging case was

Table 1
Cytotoxicity of the compounds determined for HeLa, GMK, and LF cell lines and expressed as 50% cytotoxic concentration (CC_{50}).

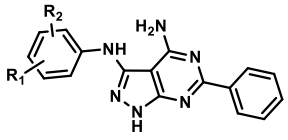

			CC_{50} (mean ± SD) towards cell lines (μM)	
Compound	R_1	R_2	HeLa	GMK
Pleconaril			36.28 ± 14.27	17.67 ± 5.01
OBR-5-340	4-CF_3	H	>270.05	>270.05
RCB04166	H	H	>165.40[a]	>330.80
RCB23137	4-Me	H	>316.06	>316.06
RCB23138	4-Cl	H	>296.91	>296.91
RCB23139	4-Br	H	9.46 ± 1.95	62.48 ± 29.64
RCB23140	4-I	H	10.14 ± 2.95	41.95 ± 5.47
RCB23141	4-F	H	>312.21	>312.21
RCB23142	H	2-F	>312.21	>312.21
RCB23143	4-F	3-F	84.71 ± 25.60	209.68 ± 5.07
RCB23144	4-F	2-F	>295.60	>295.60
RCB23145	3-F	5-F	31.39 ± 6.96	≥295.60

[a] Maximum test concentration 50 μg/ml.

Table 2
Anti-rhinovirus activity of the compounds determined in HeLa cells using a cytopathic effect inhibition assay.

	Cmpd		OBR-5-340	RCB 04166	RCB 23137	RCB 23138	RCB 23139	RCB 23140	RCB 23141	RCB 23142	RCB 23143	RCB 23144	RCB 23145
	R_1	PLC[a]	4-CF_3	H	4-Me	4-Cl	4-Br	4-I	4-F	H	4-F	4-F	5-F
	R_2		H	H	H	H	H	H	H	2-F	3-F	2-F	3-F
50% inhibitory concentration against a panel of 50 rhinovirus types (μM)[b]	A1A	0.23	57.46	29.02	16.22	30.70	7.10	n.a.[c]	25.14	n.a.	n.a.	n.a.	n.a.
	A1B	0.07	17.52	n.a.	3.16	4.43	4.23	4.39	10.64	n.a.	8.03	n.a.	3.55
	A2	0.05	30.34	n.a.	11.31	15.72	5.81	5.22	23.53	n.a.	n.a.	n.a.	n.a.
	B3	0.12	11.19	5.70	1.81	2.95	2.23	2.83	9.42	4.41	41.68	16.24	23.90
	B5[c]	n.a.	0.02[c]	0.03	0.01	0.01	0.01	0.03	0.03	0.02	0.08	0.01	0.14
	B6	0.09	108.02	n.a.	10.56	8.28	3.24	5.01	49.75	n.a.	n.a.	n.a.	n.a.
	B7	0.11	12.88	n.a.	7.59	3.86	3.17	3.02	10.44	n.a.	10.98	n.a.	3.20
	A8	3.12	7.51	n.a.	5.57	6.12	2.56	2.31	14.11	82.13	25.88	75.65	11.34
	A9	0.14	18.77	n.a.	5.34	4.17	2.04	1.89	22.86	n.a.	12.14	n.a.	6.95
	A10	0.04	45.10	n.a.	18.78	9.55	7.08	6.16	39.18	n.a.	n.a.	n.a.	n.a.
	A11	0.05	15.37	n.a.	4.03	4.08	2.42	1.46	21.50	n.a.	n.a.	n.a.	16.72
	B14	0.09	43.11	n.a.	7.02	6.98	3.29	4.89	38.61	n.a.	n.a.	n.a.	n.a.
	A15	0.2	27.74	27.35	3.43	16.82	4.98	5.42	29.70	n.a.	n.a.	n.a.	n.a.
	A16	0.15	18.34	n.a.	12.45	6.93	3.85	3.62	n.a.	n.a.	16.16	n.a.	n.a.
	B17	3.47	12.83	n.a.	4.88	1.78	1.8	2.56	11.50	n.a.	n.a.	n.a.	n.a.
	A18	0.13	1.55	9.55	1.92	1.71	1.29	1.05	10.71	33.55	4.44	18.52	13.58
	A19	0.23	58.22	n.a.	67.54	10.39	4.79	4.52	27.11	n.a.	n.a.	n.a.	n.a.
	A20	0.03	12.32	9.34	4.76	3.65	3.70	2.95	8.87	n.a.	5.86	n.a.	2.49
	A23	0.07	6.93	n.a.	10.41	4.61	5.75	n.a.	5.41	n.a.	n.a.	n.a.	2.62
	A24	0.17	13.09	n.a.	10.17	4.5	3.27	2.81	11.13	n.a.	9.77	n.a.	2.28
	A25	0.07	13.57	n.a.	16.06	6.71	4.98	3.34	5.75	n.a.	n.a.	n.a.	1.94
	A28	0.10	50.03	n.a.	46.93	n.a.	n.a.	n.a.	15.88	n.a.	26.24	n.a.	9.68
	A29	0.06	28.76	n.a.	8.05	14.38	6.39	5.91	54.25	n.a.	n.a.	n.a.	n.a.
	A30	0.19	49.17	17.56	8.84	26.37	6.28	n.a.	21.31	n.a.	n.a.	n.a.	32.02
	A39	0.15	31.72	n.a.	4.67	6.77	6.57	5.07	n.a.	n.a.	n.a.	n.a.	8.28
	A40	0.08	29.37	n.a.	11.77	5.9	5.03	3.81	16.47	113.52	21.26	n.a.	6.97
	A41	2.56	18.07	n.a.	15.99	5.43	3.29	2.84	46.98	n.a.	27.87	n.a.	15.07
	B42	n.a.	0.02	0.03	0.01	0.01	0.01	0.02	0.03	0.01	0.06	0.01	0.11
	A44	n.a.	0.42	0.03	0.04	0.03	0.08	0.14	0.12	0.05	0.42	0.04	0.27
	A46	0.17	13.30	19.06	5.61	3.37	3.25	2.52	10.65	n.a.	n.a.	n.a.	5.22
	A47	0.01	31.82	n.a.	59.88	7.00	6.17	5.51	14.99	n.a.	10.81	n.a.	5.86
	B48	n.a.	0.58	0.09	0.03	0.02	0.09	0.15	0.08	0.05	0.51	0.10	0.59
	A49	0.04	6.69	n.a.	6.06	2.09	2.52	3.48	4.62	n.a.	6.13	n.a.	1.78
	B52	7.29	11.04	6.77	2.01	0.73	0.65	2.22	2.19	2.92	n.a.	3.12	n.a.
	A54	n.a.	n.a.	n.a.	35.99	100.9	n.a.	n.a.	n.a.	n.a.	n.a.	n.a.	n.a.
	A55	0.03	n.a.	n.a.	6.49	12.56	4.87	4.43	n.a.	n.a.	n.a.	n.a.	n.a.
	A56	0.13	9.22	9.30	4.99	5.38	3.10	2.30	n.a.	n.a.	n.a.	n.a.	3.15
	A59	0.59	40.39	n.a.	9.47	33.55	6.22	6.42	35.59	n.a.	n.a.	n.a.	n.a.
	A63	0.23	55.10	n.a.	15.92	17.69	n.a.	5.64	n.a.	n.a.	n.a.	n.a.	n.a.
	A64	0.01	n.a.	n.a.	84.57	n.a.	n.a.	n.a.	n.a.	n.a.	n.a.	n.a.	n.a.
	B69	n.a.	0.28	0.02	0.01	0.02	0.04	0.12	0.02	0.01	0.08	0.02	0.22
	B70	0.40	11.33	1.64	0.11	0.3	0.38	0.74	1.67	0.47	22.03	0.72	15.47
	B72	1.24	24.90	n.a.	7.36	6.87	2.82	3.92	27.86	n.a.	n.a.	n.a.	n.a.
	A73	0.10	8.66	n.a.	6.52	6.88	2.44	n.a.	13.49	81.22	n.a.	n.a.	5.31
	A80	2.10	135.03	n.a.	58.82	32.23	n.a.	n.a.	117.78	n.a.	n.a.	n.a.	n.a.
	A81	0.32	14.48	n.a.	13.76	8.91	3.72	3.21	29.70	n.a.	30.62	n.a.	n.a.
	A85	0.01	90.96	n.a.	26.88	19.89	7.35	7.18	57.01	n.a.	n.a.	n.a.	n.a.
	B86	0.06	1.53	8.39	0.76	0.45	0.53	0.66	1.47	n.a.	5.08	2.72	10.18
	A89	0.02	26.75	n.a.	11.88	8.45	5.14	5.78	46.09	n.a.	29.81	n.a.	n.a.
	A98	1.49	22.17	10.13	13.80	17.98	6.24	5.33	17.25	n.a.	n.a.	n.a.	6.58

[a] Pleconaril; [b] The 50% inhibitory concentration was calculated from the mean dose-response curves of at least 3 independent experiments.; [c] Published RV-B5 wildtyp 1 data (Richter et al. 2024) were included for comparison. not active: less than 50% inhibition of virus-induced cytopathic effect at non-cytotoxic concentrations or at the maximal tested concentration; 50% inhibitory concentration > 10 μM; 50% inhibitory concentration >1 to 10 μM; 50% inhibitory concentration ≤ 1 μM

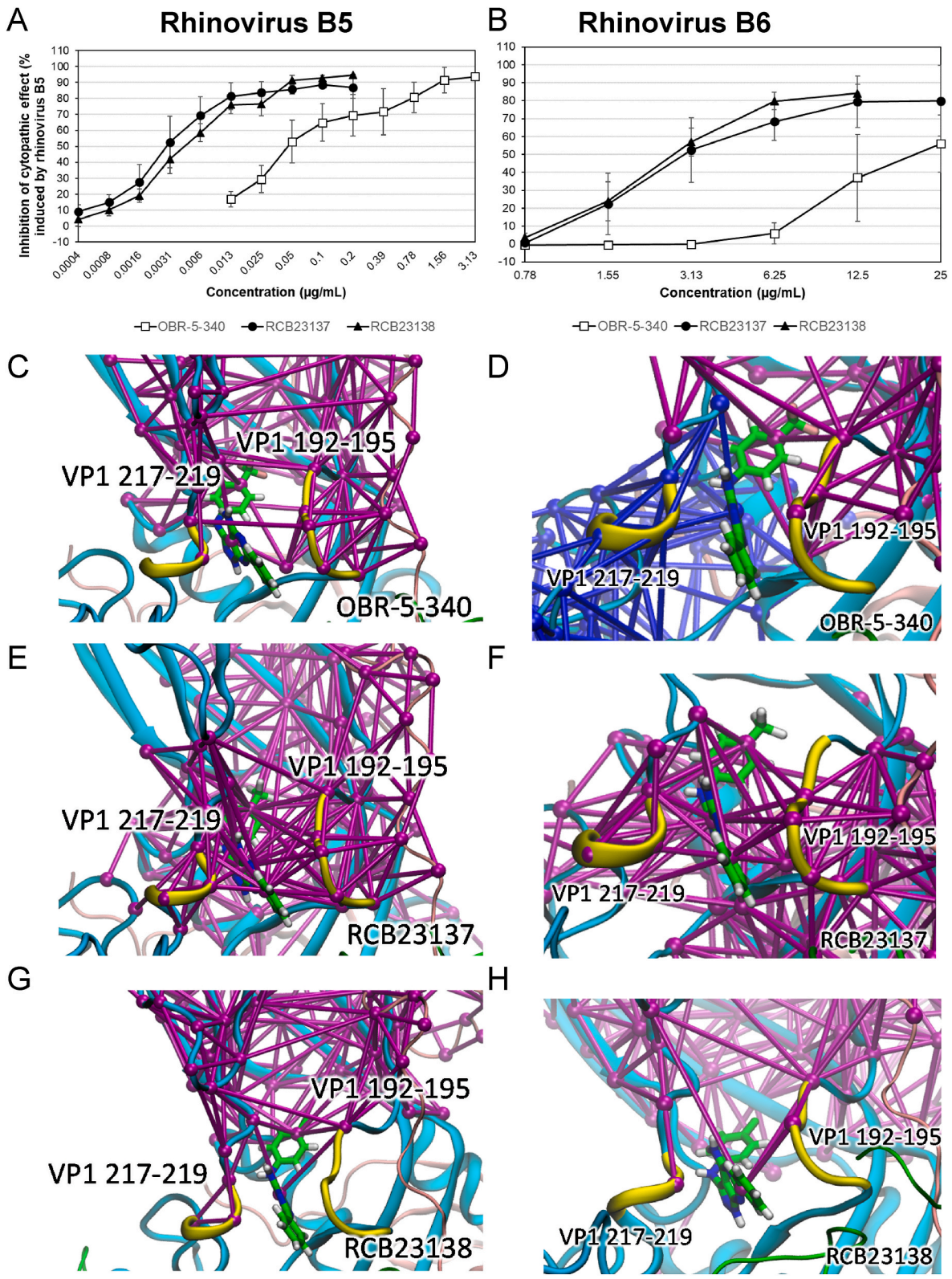

Fig. 1. Dose-response curves and complexes of RV-B5 and RV-B6 with pyrazolo[3,4-*d*]pyrimidines. **A** Dose-response curves obtained with RV-B5, highly sensitive OBR-5340, RCB23137, and RCB23138 and **B** RV-B6, sensitive to OBR-5340, RCB23137, and RCB23138. Mean values and standard deviations of at least three independent assays are shown. **C** Complex of RV-B5 and **D** RV-B6 with OBR-5-340. **E** Complex of RV-B5 and **F** RV-B6 with RCB23137. **G** Complex of RV-B5 and **H** RV-B6 with RCB23138. With the exception of **D** where the community with VP1 217–219 and another part of inhibitor is colored blue, all communities comprising loops and an inhibitor are colored violet. Viral capsid proteins are colored as follows: VP1 – cyan, VP2 – green, VP3 – pink, VP4 – grey. Loops 195–198 and 217–219 from VP1 enveloping the inhibitor are colored yellow. The atoms of inhibitors are colored accordingly: C – green, N – blue, H – white and F – pink.

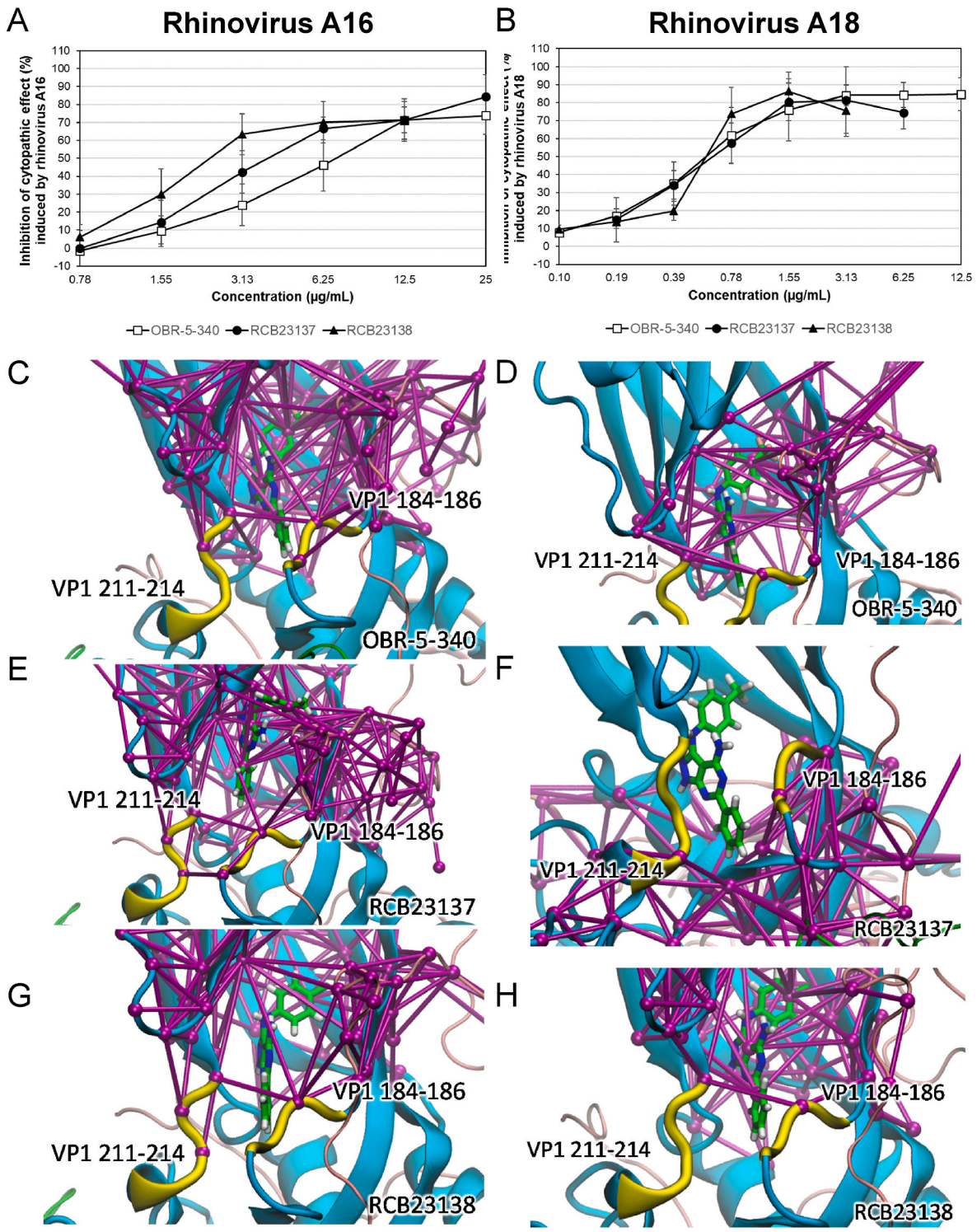

Fig. 2. Dose-response curves and complexes of RV-A16 and RV-A18 with pyrazolo[3,4-*d*]pyrimidines. **A** Dose-response curves obtained with OBR-5-340, RCB23137, and RCB23138-sensitive RV-A16 and **B** RV-A18. Mean values and standard deviations of at least three independent assays are shown. **C** Complex of RV-A16 and **D** RV-A18 with OBR-5-340. **E** Complex of RV-A16 and **F** RV-A18 with RCB23137. **G** Complex of RV-A16 and **H** RV-A18 with RCB23138. A community comprising loops and an inhibitor is colored violet (panels C–H). Viral capsid proteins are colored as follows: VP1 – cyan, VP2 – green, VP3 – pink, VP4 – grey. Loops 184–186 and 211–214 from VP1 enveloping the inhibitor are colored yellow. For inhibitors the atoms are colored accordingly: C – green, N – blue, H – white and F – pink.

discrimination of RV-A55 with different sensitivity to the selected compounds (Fig. 3A) that, in fact differ in only one substituent (4-CF_3 vs 4-Me or 4-Cl in OBR-5-340, RCB23137, and RCB23138, respectively). For the potential RV-A55-OBR-5-340 complex, we observed that only the VP1 184–186 fragment forms the same community with the OBR-5-340 (Fig. 3C). In contrast, MD simulations with RV-A55 and RCB23137 or RCB23138 demonstrated that both VP1 loops and the inhibitor belong to the same community (Fig. 3E and G). In case of RV-A64 with no (OBR-5-340 and RCB23138) or poor (RCB23137) sensitivity to the selected compounds (Fig. 3B), the inhibitor fragments comprised the same community only with one of the VP1 loops (Fig. 3D–F, H).

Overall, the MD simulations results of 18 RV-compound complexes

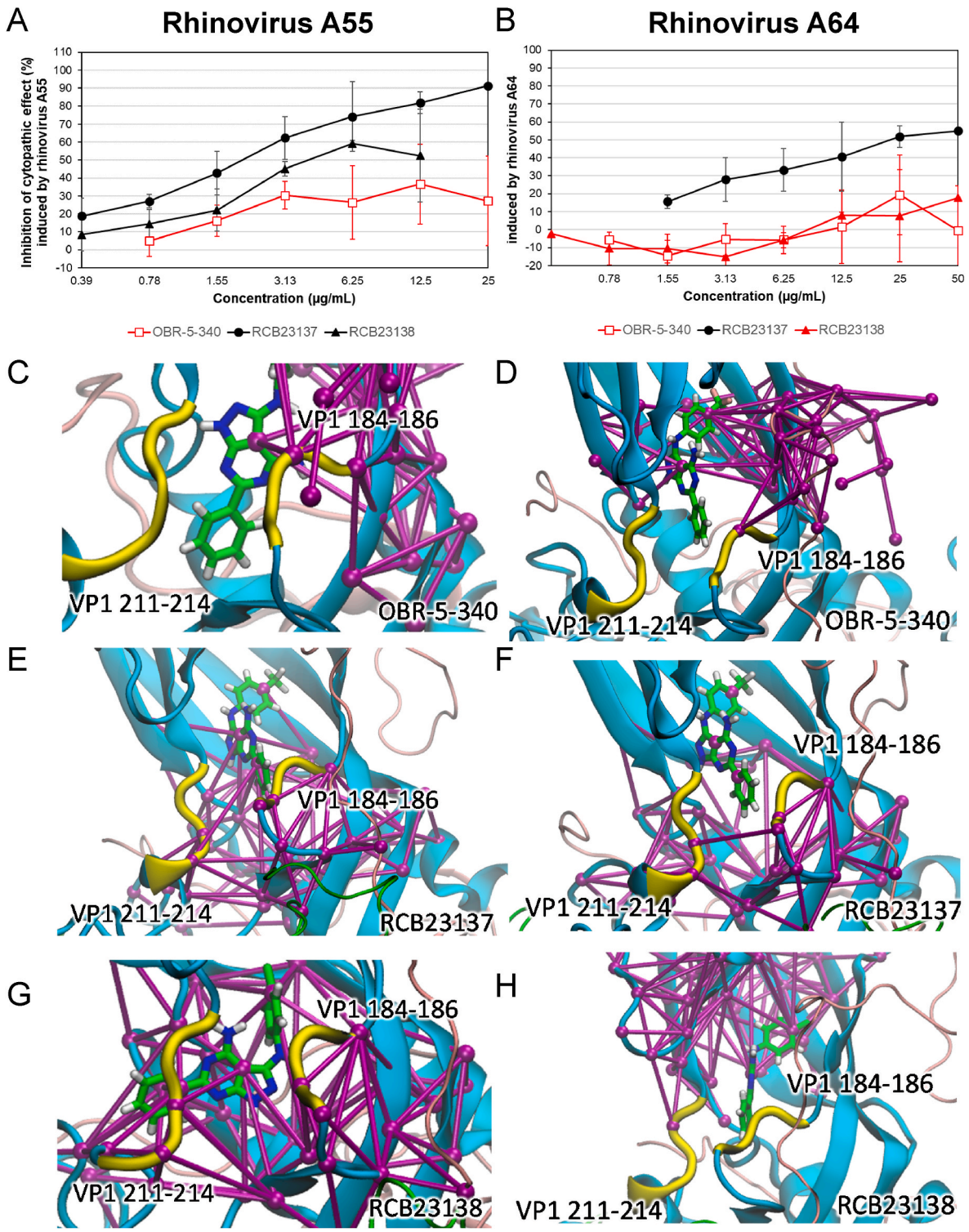

Fig. 3. Dose-response curves and complexes of RV-A55 and RV-A64 with pyrazolo[3,4-*d*]pyrimidines. **A** Dose-response curves obtained with RV-A55, insensitive to OBR-5-340, sensitive to RCB23137 and RCB23138 and **B** RV-A64, insensitive to OBR-5-340 and RCB23138, sensitive to RCB23137. Mean values and standard deviations of at least three independent assays are shown. **C** Complex of RV-A55 and **D** RV-A64 with OBR-5-340. **E** Complex of RV-A55 and **F** RV-A64 with RCB23137. **G** Complex of RV-A55 and **H** RV-A64 with RCB23138. A community comprising loops and an inhibitor is colored violet (panels C–H). Viral capsid proteins are colored as follows: VP1 – cyan, VP2 – green, VP3 – pink, VP4 – grey. Loops 184–186 and 211–214 from VP1 enveloping the inhibitor are colored. For inhibitors the atoms are colored accordingly: C – green, N – blue, H – white and F – pink.

correspond with the distinct sensitivity of the six RVs studied to OBR-5-340, RCB23137, and RCB23138. They proved our hypothesis that dynamic features of VP1 determine the activity of studied pyrazolo[3,4-d] pyrimidines against RVs (Richter et al., 2024). Dynamic network analysis is commonly utilized to determine signaling pathways to the active site upon binding of the inhibitor to the allosteric site (Cui and Karplus, 2008; Ni et al., 2017; Nussinov and Tsai, 2013). Other applications are in the field of the characterization of motion of protein parts.

More precisely, one can determine protein fragments, so-called "communities", that demonstrate correlated motion. This qualitative measure is more reliable as direct calculations of binding energies suffer from large errors (de Ruiter and Oostenbrink, 2020). To avoid these errors, we analyzed dynamic behavior of the binding site region in the viral capsid proteins of RVs and proposed criterion that can be utilized for qualitative discrimination of binding affinities. In case of strong binding, an inhibitor and two VP1 loops that envelope it belong to the same community. This can be explained by stronger binding, which means stronger interactions between the protein and ligand, likely reduce fluctuations in the corresponding interatomic distances, thereby increasing the weight of the edges connecting these fragments and grouping them into the same community.

As shown here, complexes of RVs with pyrazolo[3,4-d]pyrimidines (RV-B5, RV-B6, RV-A16, RV-A18, RV-A55, and RV-A64 with OBR-5-340, RCB23137 and RCB23138) exhibit different dynamic behavior depending on their potency. In pyrazolo[3,4-d]pyrimidine-sensitive RVs, the compound is enveloped by two VP1 loops: VP1 192–195 and VP1 217–219 for RV-B types and VP1 184–186 and VP1 211–214 for RV-A types. If a stable complex is formed, an inhibitor molecule acts like a bridge (zipper-like) between these two loops, and these molecular fragments movements are correlated. Contrary, if the complex is unstable, the compound demonstrates correlated motions with only one of two loops. For intermediate cases, loops belong to different communities, but are connected via the inhibitor. These correlations are valid for all considered compounds, *RV-A,* and *RV-B*. Herein, we derive to the conclusion that not only static interactions between the inhibitor and its target are important for the complex formation, but also, dynamic behavior determines the binding affinity, at least for these particular systems. These findings provide important information for further rational design of anti-RV capsid binders.

CRediT authorship contribution statement

Martina Richter: Writing – review & editing, Validation, Methodology, Investigation, Formal analysis. **Maria Khrenova:** Writing – review & editing, Writing – original draft, Visualization, Validation, Methodology, Investigation, Formal analysis, Data curation, Conceptualization. **Elena Kazakova:** Writing – review & editing, Validation, Investigation, Data curation. **Olga Riabova:** Writing – review & editing, Validation, Investigation, Data curation. **Anna Egorova:** Writing – review & editing, Writing – original draft, Visualization, Validation, Formal analysis. **Vadim Makarov:** Writing – review & editing, Writing – original draft, Supervision, Project administration, Funding acquisition, Formal analysis, Conceptualization. **Michaela Schmidtke:** Writing – review & editing, Writing – original draft, Validation, Supervision, Project administration, Funding acquisition, Data curation, Conceptualization.

Declaration of competing interest

The authors declare the following financial interests/personal relationships which may be considered as potential competing interests:

Grants/funding

This work was supported by the Russian Science Foundation (project number 24-15-00066) and the Dritte Patentportfolio Beteiligungsgesellschaft mbH & Co. KG (Germany).

Patents:

50 2007 006 042.9.

50 2012 017 045.1.

Data availability

Data will be made available on request.

Acknowledgements

The Russian Science Foundation (project number 24-15-00066) supported EK, OR, AE and VM.

We thank Birgit Jahn for technical support and would like to remember Dr. Birch-Hirschfeld who synthesized the primers.

Appendix A. Supplementary data

Supplementary data to this article can be found online at https://doi.org/10.1016/j.antiviral.2024.105993.

References

Barnard, D.L., Hubbard, V.D., Smee, D.F., Sidwell, R.W., Watson, K.G., Tucker, S.P., Reece, P.A., 2004. In vitro activity of expanded-spectrum pyridazinyl oxime ethers related to pirodavir: novel capsid-binding inhibitors with potent antipicornavirus activity. Antimicrob. Agents Chemother. 48, 1766–1772.

Boon, H., Meinders, A.J., van Hannen, E.J., Tersmette, M., Schaftenaar, E., 2024. Comparative analysis of mortality in patients admitted with an infection with influenza A/B virus, respiratory syncytial virus, rhinovirus, metapneumovirus or SARS-CoV-2. Influenza Other Respir Viruses 18, e13237.

Braun, H., Kirchmair, J., Williamson, M.J., Makarov, V.A., Riabova, O.B., Glen, R.C., Sauerbrei, A., Schmidtke, M., 2015. Molecular mechanism of a specific capsid binder resistance caused by mutations outside the binding pocket. Antivir. Res. 123, 138–145.

Chiodi, D., Ishihara, Y., 2023. "Magic chloro": profound effects of the chlorine atom in drug discovery. J. Med. Chem. 66, 5305–5331.

Cilloniz, C., Luna, C.M., Hurtado, J.C., Marcos, M.A., Torres, A., 2022. Respiratory viruses: their importance and lessons learned from COVID-19. Eur. Respir. Rev. 31.

Cui, Q., Karplus, M., 2008. Allostery and cooperativity revisited. Protein Sci. 17, 1295–1307.

de Ruiter, A., Oostenbrink, C., 2020. Advances in the calculation of binding free energies. Curr. Opin. Struct. Biol. 61, 207–212.

Egorova, A., Ekins, S., Schmidtke, M., Makarov, V., 2019. Back to the future: advances in development of broad-spectrum capsid-binding inhibitors of enteroviruses. Eur. J. Med. Chem. 178, 606–622.

Esneau, C., Duff, A.C., Bartlett, N.W., 2022. Understanding rhinovirus circulation and impact on illness. Viruses 14.

Feil, S.C., Hamilton, S., Krippner, G.Y., Lin, B., Luttick, A., McConnell, D.B., Nearn, R., Parker, M.W., Ryan, J., Stanislawski, P.C., Tucker, S.P., Watson, K.G., Morton, C.J., 2012. An orally available 3-ethoxybenzisoxazole capsid binder with clinical activity against human rhinovirus. ACS Med. Chem. Lett. 3, 303–307.

Groarke, J.M., Pevear, D.C., 1999. Attenuated virulence of pleconaril-resistant coxsackievirus B3 variants. J. Infect. Dis. 179, 1538–1541.

Heikkinen, T., Jarvinen, A., 2003. The common cold. Lancet 361, 51–59.

Jackson, D.J., Gern, J.E., 2022. Rhinovirus infections and their roles in asthma: etiology and exacerbations. J. Allergy Clin. Immunol. Pract. 10, 673–681.

Ledford, R.M., Patel, N.R., Demenczuk, T.M., Watanyar, A., Herbertz, T., Collett, M.S., Pevear, D.C., 2004. VP1 sequencing of all human rhinovirus serotypes: insights into genus phylogeny and susceptibility to antiviral capsid-binding compounds. J. Virol. 78, 3663–3674.

Lee, W.M., Kiesner, C., Pappas, T., Lee, I., Grindle, K., Jartti, T., Jakiela, B., Lemanske Jr., R.F., Shult, P.A., Gern, J.E., 2007. A diverse group of previously unrecognized human rhinoviruses are common causes of respiratory illnesses in infants. PLoS One 2, e966.

Lerman, A.S., Navarro Albarracin, L.F., Figari, A.B., Macias Lainez, V., Uez, O.C., 2023. Rhinovirus and metapneumovirus in patients with severe acute respiratory infection. Arch. Argent. Pediatr. 121, e202202605.

Makarov, V.A., Braun, H., Richter, M., Riabova, O.B., Kirchmair, J., Kazakova, E.S., Seidel, N., Wutzler, P., Schmidtke, M., 2015. Pyrazolopyrimidines: potent inhibitors targeting the capsid of rhino- and enteroviruses. ChemMedChem 10, 1629–1634.

Moriyama, M., Hugentobler, W.J., Iwasaki, A., 2020. Seasonality of respiratory viral infections. Annu Rev Virol 7, 83–101.

Ni, D., Song, K., Zhang, J., Lu, S., 2017. Molecular dynamics simulations and dynamic network analysis reveal the allosteric unbinding of monobody to H-ras triggered by R135K mutation. Int. J. Mol. Sci. 18.

Nussinov, R., Tsai, C.J., 2013. Allostery in disease and in drug discovery. Cell 153, 293–305.

Patick, A.K., 2006. Rhinovirus chemotherapy. Antivir. Res. 71, 391–396.

Pevear, D.C., Tull, T.M., Seipel, M.E., Groarke, J.M., 1999. Activity of pleconaril against enteroviruses. Antimicrob. Agents Chemother. 43, 2109–2115.

Renwick, N., Schweiger, B., Kapoor, V., Liu, Z., Villari, J., Bullmann, R., Miething, R., Briese, T., Lipkin, W.I., 2007. A recently identified rhinovirus genotype is associated with severe respiratory-tract infection in children in Germany. J. Infect. Dis. 196, 1754–1760.

Richter, M., Doring, K., Blaas, D., Riabova, O., Khrenova, M., Kazakova, E., Egorova, A., Makarov, V., Schmidtke, M., 2024. Molecular mechanism of rhinovirus escape from the Pyrazolo[3,4-d]pyrimidine capsid-binding inhibitor OBR-5-340 via mutations distant from the binding pocket: derivatives that brake resistance. Antivir. Res. 222, 105810.

Rollinger, J.M., Schmidtke, M., 2011. The human rhinovirus: human-pathological impact, mechanisms of antirhinoviral agents, and strategies for their discovery. Med. Res. Rev. 31, 42–92.
Royston, L., Tapparel, C., 2016. Rhinoviruses and Respiratory Enteroviruses: Not as Simple as ABC. Viruses 8.
Ruuskanen, O., Lahti, E., Jennings, L.C., Murdoch, D.R., 2011. Viral pneumonia. Lancet 377, 1264–1275.
Schonherr, H., Cernak, T., 2013. Profound methyl effects in drug discovery and a call for new C-H methylation reactions. Angew Chem. Int. Ed. Engl. 52, 12256–12267.
Simmonds, P., Gorbalenya, A.E., Harvala, H., Hovi, T., Knowles, N.J., Lindberg, A.M., Oberste, M.S., Palmenberg, A.C., Reuter, G., Skern, T., Tapparel, C., Wolthers, K.C., Woo, P.C.Y., Zell, R., 2020. Recommendations for the nomenclature of enteroviruses and rhinoviruses. Arch. Virol. 165, 793–797.
Thibaut, H.J., Lacroix, C., De Palma, A.M., Franco, D., Decramer, M., Neyts, J., 2016. Toward antiviral therapy/prophylaxis for rhinovirus-induced exacerbations of chronic obstructive pulmonary disease: challenges, opportunities, and strategies. Rev. Med. Virol. 26, 21–33.
Wald, J., Pasin, M., Richter, M., Walther, C., Mathai, N., Kirchmair, J., Makarov, V.A., Goessweiner-Mohr, N., Marlovits, T.C., Zanella, I., Real-Hohn, A., Verdaguer, N., Blaas, D., Schmidtke, M., 2019. Cryo-EM structure of pleconaril-resistant rhinovirus-B5 complexed to the antiviral OBR-5-340 reveals unexpected binding site. Proc. Natl. Acad. Sci. U. S. A. 116, 19109–19115.